# Thin Film, Near-Surface and Multi-Layer Investigations by Low-Energy $\mu^+$SR

T. PROKSCHA[1,*], E. MORENZONI[1], A. SUTER[1], R. KHASANOV[1,2],
H. LUETKENS[1,3], D. ESHCHENKO[1,2], N. GARIFIANOV[1,4],
E. M. FORGAN[5], H. KELLER[2], J. LITTERST[3],
C. NIEDERMAYER[1,6] and G. NIEUWENHUYS[7]

[1]*Paul Scherrer Institute, PSI, CH-5232 Villigen, Switzerland;*
*e-mail: thomas.prokscha@psi.ch*
[2]*Universität Zürich, CH-8057 Zürich, Switzerland*
[3]*Technische Universität Braunschweig, D-38106 Braunschweig, Germany*
[4]*Kazan Physical-Technical Institute, Kazan 420029, Russian Federation*
[5]*University of Birmingham, Birmingham B15 2TT, UK*
[6]*Universität Konstanz, D-78434 Konstanz, Germany*
[7]*Leiden University, 2300 RA Leiden, The Netherlands*

**Abstract.** At the Paul Scherrer Institute (PSI, Villigen, Switzerland) the beam of low-energy positive polarised muons (LE-$\mu^+$) with tunable energy between 0.5 and 30 keV allows the extension of the muon-spin-rotation technique ($\mu$SR) to studies on thin films and multi-layers (LE-$\mu^+$SR). The range of these muons in solids covers the near-surface region up to implantation depths of about 300 nm. As a sensitive local magnetic probe with a complementary observational time window to other techniques LE-$\mu^+$SR offers the unique possibility to gain new insights in these nano-scale objects. After outlining the current status of the LE-$\mu^+$ beam line we demonstrate the potential of this new technique by presenting the results of recent experiments: i) the direct observation of non-local effects in a superconducting Pb film, ii) the oxygen isotope effect on the in-plane penetration depth in optimally doped YBa$_2$Cu$_3$O$_{7-\delta}$, and iii) the first observation of the conduction electron spin polarisation in the Ag spacer of a Fe/Ag/Fe tri-layer.

**Key Words:** local probe, low-energy muons, multi-layers, muon-spin-rotation, thin films.

## 1. Introduction

The availability of a low-energy muon beam (LE-$\mu^+$) opens the fascinating possibility for depth dependent investigations of magnetic properties on a nanometer scale by means of a local magnetic probe. Unlike the "standard" muon-spin-rotation technique ($\mu$SR) [1] which makes use of muons with energies larger than 3 MeV – resulting in penetration depths and widths in solids of the order of fraction of mm and more, and thus limiting that technique to the study of bulk matter properties – LE-$\mu^+$ with tunable energies between 0.5 and 30 keV

---

\* Author for correspondence.

allow investigations of near-surface regions, thin films, interfaces and multi-layers up to depths of 300 nm [2].

The last decades have witnessed a steadily growing interest in thin film and multi-layer studies, because the controlled reduction of dimensionality can lead to new physical phenomena and technological applications. Techniques making use of polarised electrons, neutrons, photon and positrons are not able to provide *direct* magnetic depth sensitivity with nm resolution. Polarised LE-$\mu^+$ as a local magnetic probe offer a novel experimental tool to gain new insights in fundamental physical mechanisms.

About 10 years ago the development of a continuous LE-$\mu^+$ beam at the Paul Scherrer Institute (PSI, Villigen, Switzerland) was started to extend the well developed and established $\mu$SR technique to nanometer scale studies. The application of LE-$\mu^+$ as an extension of $\mu$SR (LE-$^+$SR) has reached now a maturity that allows its use as a standard tool in condensed matter research. Before we present recent exemplary experiments in Section 3 which demonstrate the capability of this young technique we briefly review the generation and properties of the LE-$\mu^+$ beam at PSI in Section 2.

## 2. Generation of low-energy polarised positive muons

The LE-$\mu^+$ beam at PSI is generated by moderation of a continuous 4-MeV, nearly 100%-polarised $\mu^+$ beam in a thin layer of a few hundred nanometers of a van der Waals bound cryosolid (s-Ne, s-Ar, s-$N_2$) deposited on the downstream side of a cold metal substrate [3]. Due to the lack of efficient inelastic energy loss mechanisms in these large band gap (>14 eV) insulators at epithermal energies below 50 eV, epithermal muons below that energy have a large escape depth (several tens of nanometers). Therefore, a fraction of $10^{-5}$–$10^{-4}$ of the incoming beam may escape into vacuum with a mean energy of about 20 eV and an RMS spread of same order. Since the moderation process is very fast ($\sim p$s) the initial polarisation of the $\mu^+$ is conserved [4] which is a mandatory requirement for their usage in $\mu$SR investigations. These epithermal $\mu^+$ form the source of the LE-$\mu^+$ beam, which is generated by electrostatic acceleration (by applying up to +20 kV to the electrically insulated moderator) of the epithermal $\mu^+$. The LE-$\mu^+$ are transported by electrostatic einzel lenses to the sample. The sample is located at a distance of about 2.3 m from the moderator position, after a 90° deflection by an electrostatic mirror. It is mounted electrically insulated on the cold head of a LHe flow cryostat. This allows the application of an accelerating or decelerating potential of up to ±12.5 kV to the sample. During transport the LE-$\mu^+$ pass through a special detector with an ultra-thin 2-$\mu$g/cm$^2$ carbon foil, which cause a RMS spread in energy of about 400 eV. This so-called trigger detector generates the start signal of the LE-$\mu$SR measurement by deflecting secondary electrons – released by the muons when passing through the carbon foil – onto a microchannel plate detector. The high-intensity continuous $\mu^+$ beams at PSI

with a currently useable rate of $3 \times 10^{7}$/s for LE-$\mu^{+}$ production translates into a LE-$\mu^{+}$ rate of about 3000/s at the moderator. Of these, up to 1000/s reach the sample position. Accepted good event rates range between 100/s and 500/s, depending on the experimental conditions such as LE-$\mu^{+}$ energy, sample and setup geometry. The mean implantation energy can be varied between 0.5 and 32 keV by choosing the appropriate high voltages at the moderator and the sample. Due to the energy spread of 400 eV the time resolution is limited to 5 ns. For details, we refer to [2, 5, 6].

## 3. Applications

The knowledge of the shape of the stopping distribution of LE-$\mu^{+}$ is a prerequisite for applications in *depth-resolved* studies on thin films and multi-layers. Note, that not all LE-$\mu^{+}$SR experiments require necessarily detailed information about the stopping distribution: for example, in studies of the energy dependence of muon charge differentiation in insulators [7], or in muon diffusion experiments in metal layers with thicknesses of order 30 nm [8] the details of the stopping distribution are of minor importance. In cases, where detailed knowledge about the implantation profile is mandatory the Monte-Carlo simulation TRIM.SP [9] can be used to calculate the stopping profile with sufficient accuracy for LE-$\mu$SR investigations [10]. This procedure has been utilised in experiments to determine the magnetic profile beneath the surface of a superconductor in the Meissner state. We describe briefly two recent studies that addressed different physical questions: the direct observations of non-local effects in Pb and the oxygen isotope effect in optimally doped $YBa_2Cu_3O_{7-\delta}$. In these experiments the muon implantation depth is controlled by the variation of the muon energy, and the magnitude of field is determined by the muon-spin precession frequency. As a last example the sensitivity of $\mu^{+}$ is used to probe for the first time the spatially oscillating conduction electron spin polarisation in the non-magnetic Ag spacer of a Fe/Ag/Fe trilayer.

### 3.1. DIRECT OBSERVATION OF NON-LOCAL EFFECTS IN Pb

The electromagnetic response of a superconductor results in the expulsion of the magnetic field beneath the surface on a scale of several 10 to several 100 nanometers (Meissner–Ochsenfeld effect). The spatial field dependence $B(z)$ – with $z$ the distance to the surface – yields valuable information about its nature. If the Cooper pairs can be treated as point-like the field penetrates exponentially with a typical length $\lambda_{\mathrm{L}}$ (London penetration depth): this is the result of the well known *local* relationship

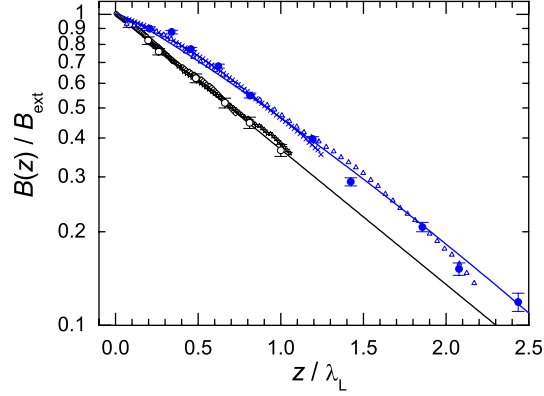$$j(\boldsymbol{r}) = -\frac{1}{\mu_0 \lambda_{\mathrm{L}}^2} A(\boldsymbol{r}) \tag{1}$$

*Figure 1. Upper data set*: measured magnetic penetration profile $B(z)$ on a logarithmic scale of Pb in the Meissner state at $T = 3.05$ K ($T_c = 7.21$ K), external field $B_{ext} = 8.8$ mT. The shape clearly deviates from exponential. *Lower data set*: $B(z)$ in YBa$_2$Cu$_3$O$_{7-\delta}$ at 20 K ($T_c = 87.5$ K): for an extreme type-II superconductor ($\xi \ll \lambda_L$) such as YBCO the local description manifested in the purely exponential shape of $B(z)$ applies. The *solid lines* represent fits to the data.

between the supercurrent density $j(\mathbf{r})$ and the vector potential $A(\mathbf{r})$, where $\mu_0$ is the permeability of vacuum. In general, the relationship is more complex allowing for a variation of the magnetic field over the size of a Cooper pair. This non-local effects are important, for example, in conventional type-I superconductors like Pb, where the coherence length $\xi > \lambda_L$ [11, 12]. In this case, the field penetrates non-exponentially into the superconductor. A direct experimental verification of this BCS prediction has been lacking up to now. Using LE-$\mu^+$ we were able to observe directly for the first time the non-exponential shape of $B(z)$ in Pb [13], see Figure 1, which represents a direct, model-independent proof of the non-local response of Pb. The Pb samples with thicknesses 1055(50) nm and 430(20) nm were sputtered onto a sapphire disk with 50 mm diameter where the thickness was controlled offline by RBS. Thin oxide layers of 6 and 16 nm were found, respectively. The critical temperature $T_c = 7.21(1)$ K was determined by means of resistivity and susceptibility measurements. After zero-field cooling the samples an external field $B_{ext} = 8.8$ mT was applied parallel to the sample surface. For the Pb data the analysis yields $\xi^{Pb} = 90(5)$ nm and $\lambda_L^{Pb} = 57(2)$ nm for $T = 0$ K. For comparison, data of the type-II superconductor YBa$_2$Cu$_3$O$_{7-\delta}$ are shown in Figure 1 as well. The profile is purely exponential, as expected, and the analysis yields $\lambda_L^{YBCO} = 146(3)$ nm for T = 0 K.

## 3.2. OXYGEN ISOTOPE EFFECT IN YBa$_2$Cu$_3$O$_{7-\delta}$

By means of LE-$\mu^+$SR the penetration depth can be determined to an accuracy of better than 1%. This allows investigations of small effects on the penetration depth in the high-temperature superconductor (HTSc) YBa$_2$Cu$_3$O$_{7-\delta}$ due to complete oxygen isotope exchange. Up to now a theory describing the pairing

mechanism in HTSc's is still missing, and one of the open questions is, if the supercarriers couple to the lattice. The measurement of $\lambda_L$ is well suited for that study in optimally doped $YBa_2Cu_3O_{7-\delta}$, because it is directly related to the effective mass $m^*$ of the supercarriers:

$$1/\lambda^2 = \mu_0 e^2 n_s / m^*, \tag{2}$$

where $e$ is the elemental charge and $n_s$ the superconducting charge carrier density. Another important parameter of a superconductor, the superconducting transition temperature $T_c$, shows only a tiny oxygen-isotope shift in optimally doped $YBa_2Cu_3O_{7-\delta}$. In a recent experiment the oxygen-isotope effect on the in-plane penetration depth $\lambda_L^{ab}$ was directly measured by means of LE-$\mu^+$SR [14]. In this measurement the $^{16}O$ of the sample was completely substituted by $^{18}O$, and $\lambda_L^{ab}$ was measured before and after oxygen-exchange. It is found that $\lambda_L^{ab}$ is 2.8(1.0)% larger in the $^{18}O$ substituted sample. There is strong evidence that this is mainly an effect due to a change of $m_{ab}^*$, since an independent NQR measurement reveals that $n_s$ does not change due to oxygen substitution. The result indicates that the mass of the superconducting carriers is not decoupled from the lattice in optimally doped cuprate superconductors. This is not expected in a BCS model within the adiabatic Migdal approximation, which is applicable for most of the classical superconductors.

### 3.3. CONDUCTION ELECTRON SPIN POLARISATION IN THE Ag SPACER OF A Fe/Ag/Fe TRILAYER

The capability of controlled growth of heterostructures on a nanometer scale opened the possibility of tailoring materials with new physical properties. In particular, multi-layers of magnetic and non-magnetic materials led to the discovery of new physical phenomena, such as giant magnetoresistance (GMR) [15] or the interlayer exchange coupling (IEC) [16]. The IEC between two ferromagnetic films separated by a non-magnetic intermediate layer depends on the spacer thickness: it oscillates and changes sign when varying the thickness. Theoretical approaches to describe IEC are RKKY and quantum-well models. The magnetic coupling between the two magnetic layers is mediated by the induced spin-polarisation of conduction electrons in the non-magnetic layer. This polarisation is hardly accessible experimentally because it rapidly decays with increasing distance $x$ to the magnetic interface, and because of its smallness compared to the large magnetic moments of the magnetic layers. This requires a local magnetic probe with large sensitivity. The LE-$\mu^+$SR technique offers this sensitivity and is capable to investigate the non-magnetic layer sandwiched between the ferromagnetic films by selective implantation of the muons in the spacer. This has been demonstrated in a recent experiment [17] where for the first time the conduction electron spin polarisation has been measured in the Ag layer of an epitaxial 4 nm Fe/20 nm Ag/4 nm Fe(001) trilayer on a MgO(001)
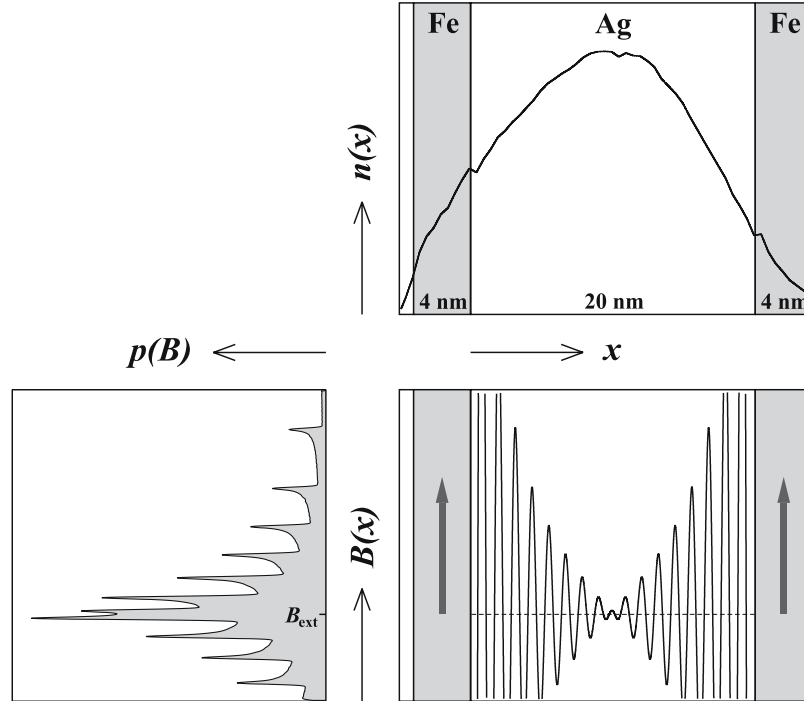
*Figure 2.* Principle of the LE-$\mu^+$SR measurement of the oscillating electron spin polarisation in the Ag intermediate layer of a 4 nm Fe/20 nm Ag/4 nm Fe(001) film on a MgO(001) substrate. The maximum of the muon stopping profile $n(x)$ is placed close to the centre of the Ag layer by proper adjustment of the LE-$\mu^+$ energy. The field distribution $p(B)$ as measured by the muon ensemble directly reflects the oscillating polarisation in the Ag spacer which is proportional to the local field $B(x)$ sensed by the $\mu^+$. The distinct peaks in $p(B)$ correspond to maxima or minima of the oscillating $B(x)$.

substrate. The principle of the measurement is shown in Figure 2. The sample was first magnetised at room temperature in a field of 0.1 T. In the remnant state it was then cooled to 20 K before applying a field of 8.8 mT parallel to the easy axis and parallel to the sample surface to carry out the LE-$\mu^+$SR measurements. The implantation energy was 3 keV to stop most of the muons in the Ag layer. The experimental data are in good agreement with the theoretical shape of $p(B)$ shown in Figure 2. The fit of the theoretical $p(B)$ to the data yields an attenuation of $x^{-0.8(1)}$ of the oscillating polarisation in the Ag layer perpendicular to the interface. Here, the local magnetic field $B_{\mathrm{loc}}(x)$ as sensed by the muon is modelled by the superposition of the magnetic field profiles induced by each of the two Fe/Ag interfaces [$B_{\mathrm{loc}}(x) = B(x) + B(D - x)$, $D = 20$ nm the Ag layer thickness]. The observed attenuation indicates a different spatial dependence than the IEC which follows $x^{-2}$. This unexpected result cannot be explained within a RKKY description of IEC. It may be explained in a theory that considers the full confinement of the electrons within the intermediate layer, as it was found for the Co/Cu/Co trilayer [18].

## 4. Outlook

Over the past years the continuous developments on the surface muon beam line, the epithermal muon source and the LE-$\mu^+$ apparatus have led to a steady increase of the LE-$\mu^+$ flux at the sample up to 1000/s. This affords LE-$\mu^+$SR as a serious tool for condensed matter investigations. However, this novel technique is still limited in statistics, especially if compared with the intensities of several tens of kilohertz available at existing $\mu$SR facilities. It is therefore evident that an intensity increase of the LE-$\mu^+$ rate is of primary importance. A significant straightforward advancement can not be expected by improvements of the existing setup, whereas a corresponding increase of the surface muon flux can lead to an enhancement by one order of magnitude. A new, large-acceptance surface muon beam line is currently under construction at PSI and will be ready for user operation in 2005. It was specially designed for the generation of a low-energy muon beam [19]. The new beam line will yield a raise of LE-$\mu^+$ rate by a factor of seven, thus allowing the full exploitation of the potential of polarised muons as nano-scale probes.

## Acknowledgements

## References

1. Blundell S. J., *Cont. Phys.* **40** (1999), 175.
2. Bakule P. and Morenzoni E., *Cont. Phys.* **45** (2004), 203.
3. Harshman D. R., Mills Jr. A. P., Beveridge J. L., Kendall K. R., Morris G. D., Senba M., Warren J. B., Rupaal A. S. and Turner J. H., *Phys. Rev. B* **36** (1987), 8850.
4. Morenzoni E., Kottmann F., Maden D., Matthias B., Meyberg M., Prokscha T., Wutzke T. and Zimmermann U., *Phys. Rev. Lett.* **72** (1994), 2793.
5. Morenzoni E., Glückler H., Prokscha T., Weber H. P., Forgan E. M., Jackson T. J., Luetkens H., Niedermayer C., Pleines M., Birke M., Hofer A., Litterst J., Riseman T. and Schatz G., *Physica B* **289**–**290** (2000), 653.
6. Prokscha T., Morenzoni E., David C., Hofer A., Glückler H., Scandella L., *Appl. Surf. Sci.* **172** (2001), 235.
7. Prokscha T., Morenzoni E., Garifianov N., Glückler H., Khasanov R., Luetkens H., Suter A., *Physica B* **326** (2003), 51.
8. Luetkens H., Korecki J., Morenzoni E., Prokscha T., Garifianov N., Glückler H., Khasanov R., Litterst J., Slezak T., Suter A., *Physica B* **326** (2003), 545.
9. Eckstein W., *Computer Simulation of Ion-Solid Interactions*, Springer, Berlin, Heidelberg New York, 1991.
10. Morenzoni E., Glückler H., Prokscha T., Khasanov R., Luetkens H., Birke M., Forgan E. M., Niedermayer C. and Pleines M., *NIM B* **192** (2002), 254.

11. Pippard A. B., *Proc. R. Soc. London, A* **216** (1953), 547.
12. Bardeen J., Cooper L. N. and Schrieffer J. R., *Phys. Rev.* **108** (1957), 1175.
13. Suter A., Morenzoni E., Khasanov R., Luetkens H., Prokscha T. and Garifianov N., *Phys. Rev. Lett.* **92** (2004), 087001.
14. Khasanov R., Eshchenko D. G., Luetkens H., Morenzoni E., Prokscha T., Suter A., Garifianov N., Mali M., Roos J., Conder K. and Keller H., *Phys. Rev. Lett.* **92** (2004), 057602.
15. Baibich M. N., Broto J. M., Fert A., Nguyen Van Dau F., Petroff F., Eitenne P., Creuzet G., Friederich A. and Chazelas J., *Phys. Rev. Lett.* **61** (1988), 2472.
16. Grünberg P., Schreiber R., Pang Y., Brodsky M. B. and Sowers H., *Phys. Rev. Lett.* **57** (1986), 2442.
17. Luetkens H., Korecki J., Morenzoni E., Prokscha T., Birke M., Glückler H., Khasanov R., Klauss H. H., Slezak T., Suter A., Forgan E. M., Niedermayer C. and Litterst F. J., *Phys. Rev. Lett.* **91** (2003), 017204.
18. Mathon J., Umerski A., Villeret M. and Muniz R. B., *Phys. Rev.* **B59** (1999), 6344.
19. Prokscha T., Morenzoni E., Deiters K., Foroughi F., George D., Kobler R. and Vrankovic V., these proceedings.